The South American Land Data Assimilation System (SALDAS) 5-Yr Retrospective Atmospheric Forcing Datasets

LUIS GUSTAVO G. DE GONCALVES,* WILLIAM J. SHUTTLEWORTH,+ DANIEL VILA,# ELIANE LARROZA,@ MARCUS J. BOTTINO,@ DIRCEU L. HERDIES,@ JOSE A. ARAVEQUIA,@ JOAO G. Z. DE MATTOS,@ DAVID L. TOLL,& MATTHEW RODELL,& AND PAUL HOUSER**

*Earth System Science Interdisciplinary Center, University of Maryland, College Park, College Park, and Hydrological Sciences Branch, NASA Goddard Space Flight Center, Greenbelt, Maryland
+Department of Hydrology and Water Resources, The University of Arizona, Tucson, Arizona
#Cooperative Institute of Climate Studies, and Earth System Science Interdisciplinary Center, University of Maryland, College Park, College Park, Maryland
@Centro de Previsão de Tempo e Estudos Climáticos/Instituto Nacional de Pesquisas Espaciais, Cachoeira Paulista, São Paulo, Brazil
&Hydrological Sciences Branch, NASA Goddard Space Flight Center, Greenbelt, Maryland
**Center for Research on Environment and Water, Institute of Global Environment and Society, Calverton, Maryland

(Manuscript received 29 April 2008, in final form 24 February 2009)

ABSTRACT

The definition and derivation of a 5-yr, 0.125°, 3-hourly atmospheric forcing dataset that is appropriate for use in a Land Data Assimilation System operating across South America is described. Because surface observations are limited in this region, many of the variables were taken from the South American Regional Reanalysis; however, remotely sensed data were merged with surface observations to calculate the precipitation and downward shortwave radiation fields. The quality of this dataset was evaluated against the surface observations available. There are regional differences in the biases for all variables in the dataset, with volumetric biases in precipitation of the order 0–1 mm day^{-1} and RMSE of 5–15 mm day^{-1}, biases in surface solar radiation of the order 10 W m^{-2} and RMSE of 20 W m^{-2}, positive biases in temperature typically between 0 and 4 K depending on the region, and positive biases in specific humidity around 2–3 g kg^{-1} in tropical regions and negative biases around 1–2 g kg^{-1} farther south.

1. Introduction

Land surface models (LSMs) are an important component of numerical weather prediction (NWP) and global climate models and can also be used to assess surface hydrology. They provide a description of the soil–vegetation system that is the lower boundary condition on the atmosphere and feedback from the underlying land surface. Several studies have shown that surface storage of water and energy is important in land–atmosphere systems at regional and global scale (e.g., Betts et al. 1996; Koster and Suarez 1999; Fennessey and Shukla 1999; Koster et al. 2004; de Goncalves et al. 2006a), and that surface states such as soil moisture and temperature can affect atmospheric numerical model predictions.

There are continuing efforts to increase the accuracy (and, as a result, complexity) of the representation within LSMs of the processes involved in the soil–vegetation–atmosphere system. However, realism can only ensue if LSMs are provided with realistic forcing data. Such forcing data typically comprises air temperature and humidity, wind speed, surface pressure, radiation, and precipitation, although the nature of the forcing variables varies with the LSM and its application. Atmospheric forcing data may be provided from surface and remotely sensed observations or may be

Corresponding author address: Luis Gustavo de Goncalves, Code 614.3, NASA Goddard Space Flight Center, Greenbelt Rd., Greenbelt, MD 20771.
E-mail: luis.g.degoncalves@nasa.gov

DOI: 10.1175/2009JHM1049.1

© 2009 American Meteorological Society

model derived, or may be a combination of these two options. Land Data Assimilation Systems (LDASs; Mitchell et al. 2004) have been successfully used to provide improved initial soil moisture fields in near–real time for use in predictive meteorological models and to address land management issues. LDASs comprise two-dimensional arrays of LSMs that are set up to correspond to the grid squares used in the predictive model, and then forced by model-derived near-surface fields supplemented to the maximum extent possible by observations of meteorological variables.

When implementing LDAS, the scarcity of land surface data at the spatial and temporal resolutions at which the LDAS operate is an important challenge (Maurer et al. 2002). Providing adequate observations of precipitation is particularly problematic because precipitation is so variable spatially and it often points sample data from well-separated rain gauges that are the only data available. Some regions of the globe (e.g., North America, Europe, and Japan) have reasonably dense observational coverage. Other regions, including South America, do not. The rain gauge data available in South America are very sparse and strongly biased toward more populated areas near the edge of the continent or near inland cities along the main river courses (de Goncalves et al. 2006b). Consequently, LDAS modelers are obliged to rely heavily on atmospheric analyses and remote sensing products for rainfall forcing (Rodell et al. 2004).

This paper describes the creation and validation of the forcing datasets used with the South American Land Data Assimilation System (SALDAS; data are available online at http://lba.cptec.inpe.br/beija-flor/). The SALDAS dataset has also been adopted as the regional forcing data for the model comparisons currently being made under the Large-scale Biosphere–Atmosphere Experiment in Amazonia (LBA) Model Intercomparison Study (MIP; see protocol at http://www.climatemodeling.org/lba-mip/).

2. SALDAS forcing data

The SALDAS forcing data are derived by combining model calculated fields and observations to produce the distributed atmospheric fields needed for land surface modeling across the entire continent of South America.

a. Model-calculated data

Model-calculated values of air temperature, wind speed, and specific humidity at 2 m, surface pressure, downward shortwave and longwave surface radiation, and precipitation are available from the South American Regional Reanalysis (SARR). These SARR datasets (Aravéquia et al. 2008) were released in 2006 by the Centro de Previsão de Tempo e Estudos Climáticos [CPTEC (Center for Weather Forecast and Climate Studies)], a division of the Instituto Nacional de Pesquisas Espaciais [INPE (Brazilian National Institute for Space Research)]. The datasets consist of dynamically consistent, high-resolution, high-frequency, atmospheric data over South America. Currently, the SARR is available for a 5-yr period from 2000 to 2004.

Data assimilation provides estimates of variables important in the hydrological cycle that are more accurate and consistent than observations alone. The SARR data are derived using the Regional Physical-space Statistical Analysis System (RPSAS) data assimilation scheme applied at 40-km horizontal resolution and 38 vertical levels with a modified version of the National Centers for Environmental Prediction (NCEP) Eta Model (Chou and Herdies 1996). This system integrates upper air and surface observations from several sources over South America in real time and, when applied in reanalysis mode, it allows for assimilation of additional observations, including vertical soundings from the Radiation, Cloud, and Climate Interactions (RACCI)/LBA Amazon field campaigns and South American Low-Level Jet Experiment (SALLJEX) field studies in the region of the low-level jet along the Andes.

The topography used in the Eta Model used to calculate the SARR differs substantially from the SALDAS topography, the latter being derived from the U.S. Geological Survey (USGS) global 30 arc-second (GTOPO30) elevation map (Row et al. 1995). Significant adjustment of air temperature, humidity, surface pressure, and downward longwave radiation is therefore required when deriving the SALDAS forcing data. In the Eta model, topography is represented as occurring in steps (Bryan 1969) at grid boundaries to preserve conserved properties in finite difference schemes (Mesinger et al. 1988). Consequently, the required elevation corrections are greatest in the Andes where altitude changes rapidly and step changes in Eta coordinates are greatest. The 2-m air temperature and surface pressure are adjusted from the Eta Model to the SALDAS elevations using standard atmospheric lapse rates, while specific humidity is adjusted assuming a constant relative humidity at these two levels. Longwave radiation is corrected using the Stefan–Boltzmann equation applied with the different corrected temperature and vapor pressure at the two levels. For greater detail, refer to Cosgrove et al. (2003). Figure 1 shows that longwave radiation corrections are fewer than 20 W m^{-2} in regions where there are no abrupt changes in topography but are greater in the Andes where they can exceed 100 W m^{-2}. Similarly, corrections in surface pressure, specific humidity, and temperature in mountainous regions can be up to 200 hPa, 10 g kg^{-1}, and 20 K,

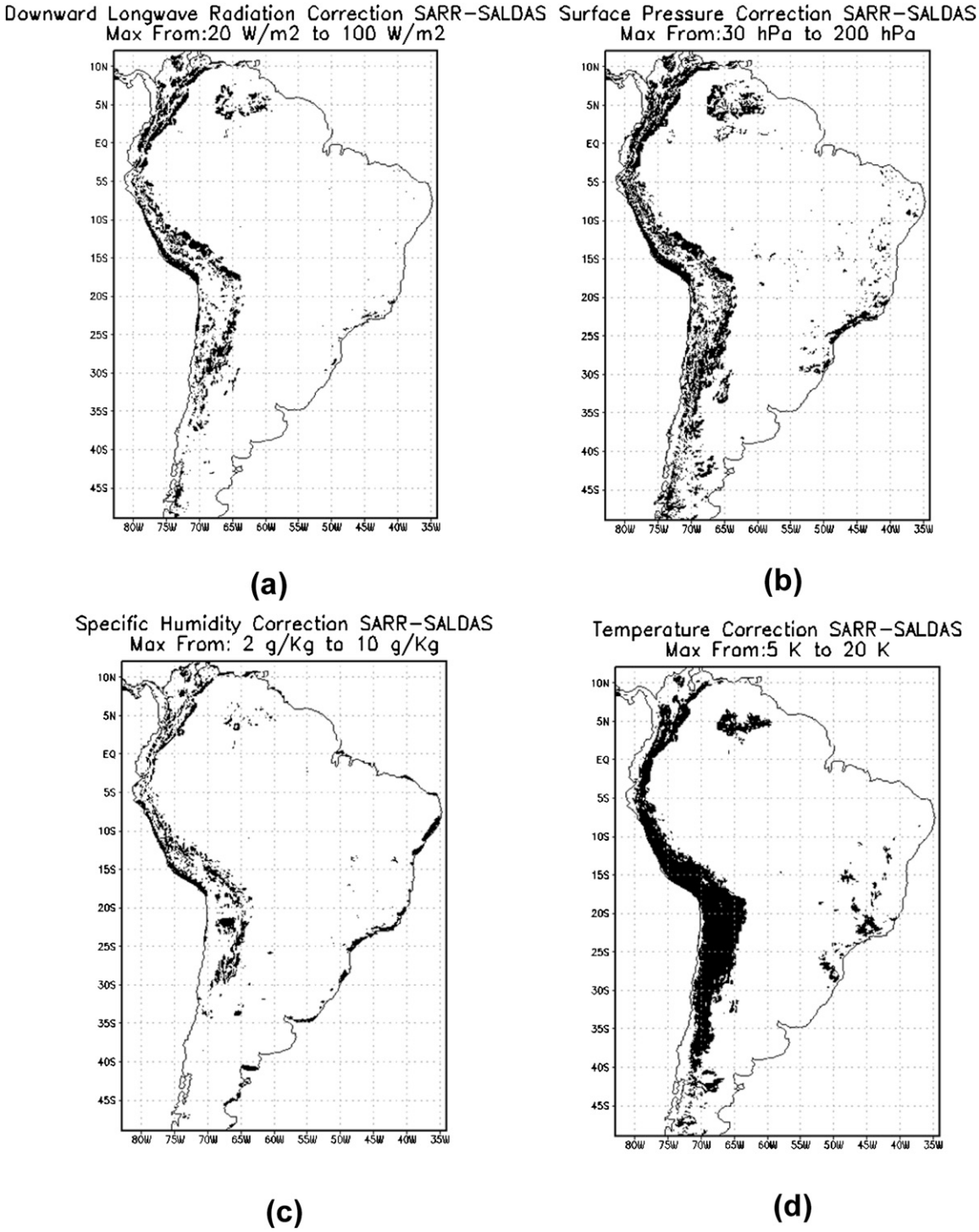

FIG. 1. Elevation corrections between SARR Eta vertical coordinates and the SALDAS topography for (a) downward longwave radiation at surface, (b) surface pressure, (c) surface specific humidity, and (d) surface air temperature. Shaded areas are where the corrections exceed minimum threshold values of 20 W m^{-2}, 30 hPa, 2 g kg^{-1}, and 5 K for downward longwave radiation, surface pressure, surface air specific humidity, and surface air temperature, respectively.

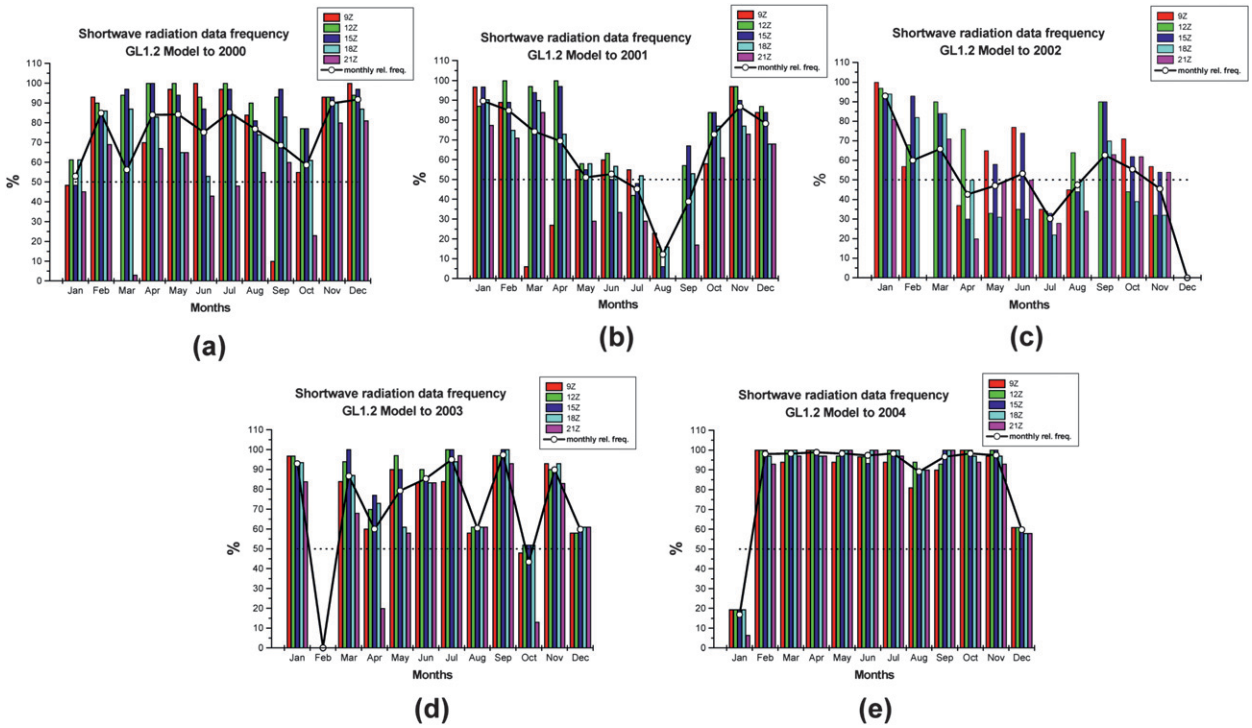

FIG. 2. Monthly percentage of GOES/GL 1.2 satellite retrievals that contributed to SALDAS forcing downward shortwave radiation data for (a) 2000, (b) 2001, (c) 2002, (d) 2003, and (e) 2004. The colored bars are the monthly average for 3-h periods within the day, and the black bar is the monthly average all-day value.

respectively, but are otherwise less than 30 hPa, 2 g kg^{-1}, and 5 K, respectively.

b. Downward shortwave radiation

When possible, the SALDAS dataset seeks to provide more realistic and accurate data over South America than that already available from existing global reanalyzes. Consequently, surface solar radiation fluxes were derived using satellite radiance measurements from a Geostationary Operational Environmental Satellite (*GOES-8*). Visible imagery was appropriately adjusted as a function of the hour of the day and latitude to follow the zenithal angle. Surface radiation was then calculated using the GL1.2 model (Ceballos et al. 2004), which was developed at the Divisao de Satelites e Sistemas Ambientais [DSA (the Division for Satellites and Environmental Systems at CPTEC/INPE)]. The GL1.2 model considers tropospheric radiative transfer in two broadband spectral intervals. Ultraviolet and visible radiations are considered nonabsorbing, while near-infrared radiation is assumed to undergo negligible atmospheric scattering but has very low cloud transmittance. The current version of the GL1.2 model does not include the effect of aerosols.

The values calculated using GL1.2 were transposed from their standard 4-km grid and 30-min temporal resolution to the 0.125° and 3-h interval used in SALDAS. Data derived from the GL1.2 model are not always available and when this happens, SARR estimates of downward shortwave radiation are substituted in SALDAS. Figure 2 shows the monthly average percentage availability of satellite-derived solar radiation data in the SALDAS dataset for the period 2000–04 for 3-h periods within the day and the all-day average. The values range from 100% to 0% (e.g., in February 2003) with some variability between 3-hourly periods in the same month, especially prior to January 2004 when data availability became more stable. DSA is currently reprocessing the GL1.2 data, and the percentage availability of the satellite-derived downward shortwave radiation data in the SALDAS forcing dataset is expected to increase as a result.

c. Precipitation

The SALDAS precipitation data are primarily taken from the real-time version of the Tropical Rainfall Measuring Mission (TRMM) Multisatellite Precipitation Analysis retrievals (TMPA-RT; Huffman et al. 2007) linearly interpolated in space and time to 1/8° resolution and 3-hourly frequency. The TMPA-RT retrieval algorithm has been shown to approximately reproduce the histogram of precipitation of surface observations and

also to be reasonably effective in detecting large events at the daily time scale (Huffman et al. 2007). However, J. R. Rozante, CPTEC/INPE, 2008, (personal communication) showed that although 70% of TRMM rainfall estimates correlates with observations with correlation coefficients in the range of 0.50–0.75 (the remainder of the estimates are less than 0.5), TRMM estimates can underestimate precipitation by up to 50%, and they have poor correlation (<0.3) in regions with warm clouds, particularly during the austral winter.

To reduce bias in the satellite rainfall retrievals, they are combined with surface rain gauge observations in SALDAS, and the TMPA-RT data were selected partly because they are not already influenced by such gauge data. The merging technique used, the Combined Scheme (CoSch), uses a weighted average of additive and multiplicative corrections to remove the volume bias of satellite retrievals. For greater detail, refer to Vila et al. (2009). The daily surface precipitation observations include the data provided by the World Meteorological Organization (WMO), supplemented by data compiled by INPE from the following agencies:

1) Agência Nacional de Energia Eléctrica [ANEEL (National Agency for Electrical Energy)],
2) Agência Nacional de Águas [ANA (National Water Agency)],
3) Fundação Cearense de Meteorologia e Recursos Hídricos [FUNCEME (Meteorology and Hydrologic Resources Foundation of Ceará)],
4) Superintendência do Desenvolvimento do Nordeste [SUDENE (Superintendence for Development of the Northeast)],
5) Departamento de Águas e Energia Elétrica do Estado de São Paulo [DAEE (Department of Water and Electrical Energy for the State of São Paulo)], in collaboration with CPTEC/INPE,
6) Technological Institute of Paraná (SIMEPAR).

Version 6 of the TRMM 3B42 product is also available and might be considered an alternative source of precipitation data for SALDAS. In the TRMM 3B42 product, volume bias in satellite estimates is corrected at a monthly time scale using the Global Precipitation Climatology Centre (GPCC) surface station dataset. However, Vila et al. (2009) have shown that when the TRMM 3b42 product is merged with observations, TMPA-RT data are preferable for land surface modeling in South America. This is partly because of the additional observations from South American agencies and Brazilian automatic weather stations. The number of surface observations used is about 4 times that available in the GPCC dataset used to adjust the TRMM 3B42 product (see Fig. 3). Also, the CoSch technique involves a daily correction for precipitation volume bias rather than the monthly correction used in the version-6 3B42 data. Consequently, agreement is better at the daily and subdaily time scale, and the diurnal cycle is better characterized. This is an advantage for using data used with land surface models that are typically run with a less-than-hourly time step.

3. Validation studies for the SALDAS atmospheric forcing data

The validation strategy adopted in this study followed that used by Chou et al. (2005) and de Goncalves et al. (2006a). Because the SALDAS domain is large and the observations available for validation are very limited, continental South America was divided into large subregions that were selected to characterize different climate regimes. Figure 4 shows the three regions selected: the northern region, 17°S–11°N, 47°–83°W (NO); the northeastern region, 17°S–11°N, 33°–47°W (NE); and the central-south region, 47°S–17°N, 33°–83°W (CS). To evaluate the SALDAS data, surface observations were selected from the CPTEC/INPE database, which includes data from networks run by regional and national centers and agencies with private and federal jurisdiction across South America (refer to previous section). Comparisons between SALDAS data and observations were made for precipitation, shortwave downward radiation, temperature, and specific humidity. Because of important scale differences between single-point observations and model- and satellite-derived gridded datasets, monthly-mean region-average values of relative bias, root-mean-square error (RMSE), and correlation coefficient were calculated over the three large regions to make these comparisons.

a. Precipitation

It is important to recognize that several factors necessarily limit the rigor of the comparison between the SALDAS precipitation data and surface observations. Not least is the fact that the network of observations is so sparse across each of the three large regions considered. Averaging unevenly distributed gauge observations can compromise the characterization of spatial patterns of precipitation, and biases can be induced by the terrain complexity within each region. The present study acknowledges that these challenges, and resulting uncertainties, exist but because of the sparse data available, they cannot be not fully addressed in this validation study.

The cross-validation approach used to evaluate SALDAS precipitation data in this study was adapted from that of Chen et al. (2002; 2008) and is described as

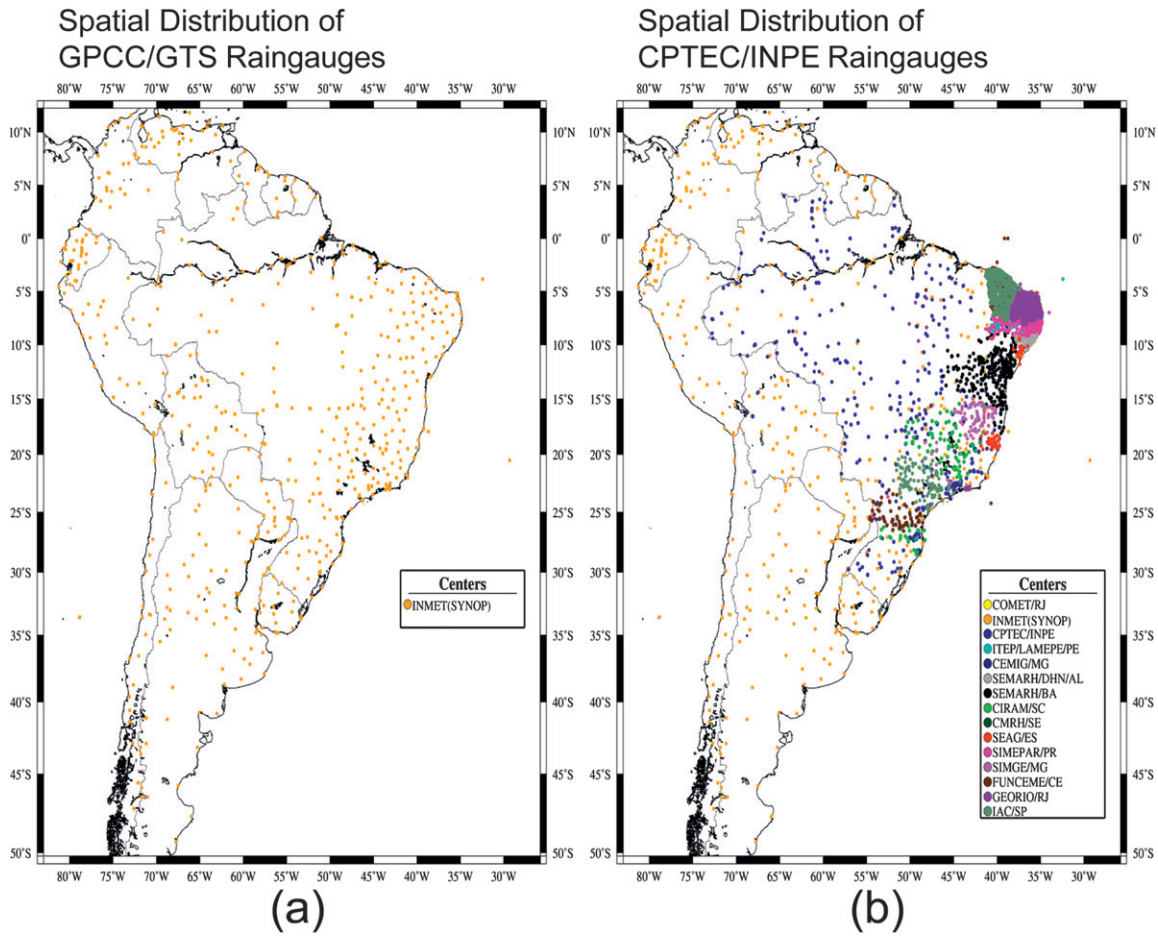

FIG. 3. Rain gauge distribution across continental South America typical of (a) the GPCC/GTS dataset and (b) the CPTEC/INPE database during the period 2000–04.

follows. Ten percent of the precipitation observations at randomly selected stations in each region were withdrawn for use in validation, while those at the remaining stations were used in the CoSch bias-removal process. This selection process was repeated 10 times with the validation data; the gauge was chosen each time from among the gauges not previously selected so that each gauge was used for validation just once. For each sample, the bias-corrected TRMM precipitation estimate was compared with the corresponding set of validation observations to evaluate the effectiveness of the CoSch bias correction (Vila et al. 2009). Mean monthly volume bias was calculated only for SALDAS grid squares where there was observed precipitation. In 2004, this evaluation of SALDAS precipitation data was also compared against a similar evaluation of the raw TRMM 3B42RT precipitation product with the same 10 subsets of observations used for validation in each sample.

Figure 5 shows the mean monthly volume bias for SALDAS and raw TRMM 3B42RT precipitation data as a function of the time of year for the three regions (NO, NE, and CS) and for the entire South American continent. The averaged monthly precipitation for the three regions and the continent are also shown. Figure 5a shows that for South America as a whole, the volume bias relative to observations in SALDAS precipitation data is substantially better than that in the raw TRMM 3B42RT precipitation data during the spring and summer in the Southern Hemisphere (i.e., in the wet season). In the winter, when there is less rainfall, the volume bias of both sets of precipitation data is small. This general result is found in all three regions, though there are differences. The SC region is most similar to South America as a whole because this is the largest region where most gauges are located. Both precipitation products show a systematic negative volume bias in the northeast region that is consistent with the results of Vila et al. (2009), but this bias is less for the SALDAS data. The volume bias in the SALDAS data is worst in the northern region. Perhaps this is because gauge stations

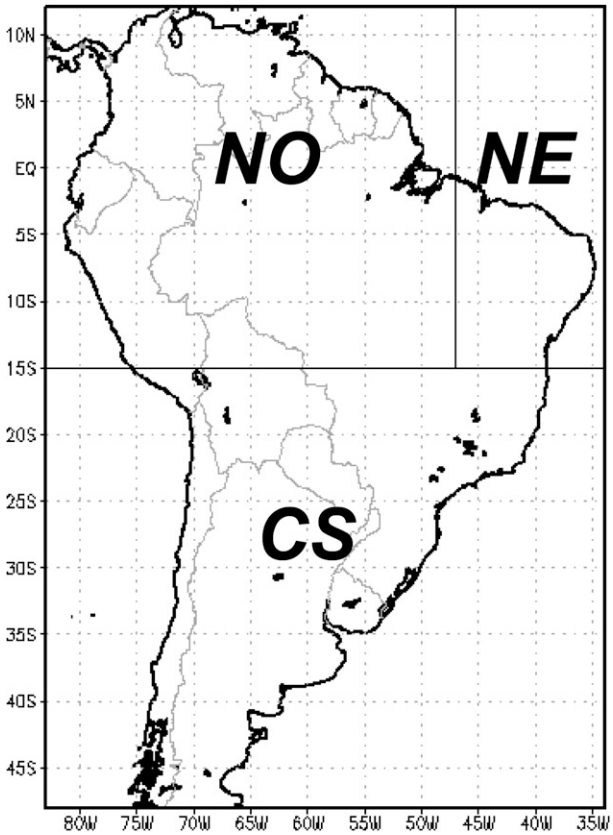

FIG. 4. The three climatic regions selected for validation studies in this analysis on basis of the prevailing annual precipitation regime.

are particularly sparse and unevenly distributed in this region and their effect within the CoSch gauge correction is less effective.

Figure 6 shows the annual variation in monthly-mean RMSE for the three regions and for South America as a whole. The SALDAS precipitation product is better than the raw TRMM 3B42RT precipitation product throughout the year, across the continent as a whole, and in all three regions separately. It is best in the southern region and not as good in the northern region. Consistent with the results found for volume bias and RSME, Fig. 7 shows the correlation coefficient for SALDAS precipitation product is also better than for the raw TRMM 3B42RT precipitation product across the continent as a whole and in all three regions.

b. Downward shortwave radiation

Ceballos et al. (2004) evaluated GL 1.2 model retrievals during 2002 against three precision pyranometers giving measured daily irradiation representative of rural, urban industrial, and urban coastal areas, and against monthly average data from 90 pyranometers in the CPTEC/INPE network. The daily mean bias of the retrievals against the precision pyranometers was around 5 W m^{-2} with a standard deviation of ~15 W m^{-2}, while the monthly means bias against the network pyranometers was approximately 10 W m^{-2} with a standard deviation of less than 20 W m^{-2}. Larger errors were found in highly industrialized and heavily agricultural areas where aerosol concentration was high.

The SALDAS downward solar radiation data are a derivative of the GL1.2 dataset, aggregated from 30 min and 0.04° resolution to 3 h and 0.125° resolution, respectively, with SARR radiation data substituted when GOES data is missing. The resulting SALDAS solar radiation data were reevaluated during 2004 in this study. Comparison was made with equivalent daily average values from the automatic station network described by Ceballos et al. (2004) over each of the CS, NE, and NO regions. Figure 8 shows the annual variation in the mean monthly bias, the standard deviation in this bias, and the RMSE. There is variation through the year but, on average, the SALDAS forcing data tend to overestimate observed radiation in the CS and NO regions and underestimate observations in the NE region. However, the correlation between SALDAS daily average solar radiation and observations also shown Fig. 8 is reasonably good, with correlation coefficients of 0.71, 0.75, and 0.82 in the NO, NE, and CS regions, respectively. Previous studies of satellite estimates of solar radiation (Whitlock et al. 1995; Pinker et al. 2001; Stackhouse et al. 2001) have reported a mean deviation of ±10 W m^{-2} with a standard deviation of less than 20 W m^{-2} for grids to the order of hundreds of square kilometers. However, for SALDAS 12 km × 12 km grid cells, the monthly-mean errors exceed these values in a few instances.

The yearly variation in solar radiation bias in the CS region has a pattern similar to that reported by Ceballos et al. (2004), with overestimation during the winter associated with higher atmospheric pollution. In the NO region, the GL1.2 (and hence, SALDAS) data overestimate observations by about 20–30 W m^{-2}. Ceballos et al. (2004) suggest this is partly due to the high concentration of aerosols during the biomass burning season, which is not included in the model, and partly due to errors in the retrieval algorithm when atmospheric precipitable water is high.

The seasonal pattern in the solar radiation bias (high in the summer and low in the winter) in the CS region is largely due to a known error in the retrieval algorithm. This error induced a systematic bias that is a function of the solar constant and Julian day and of the order −7% in January to +7% in July. There is additional error when SARR estimates are used to replace missing

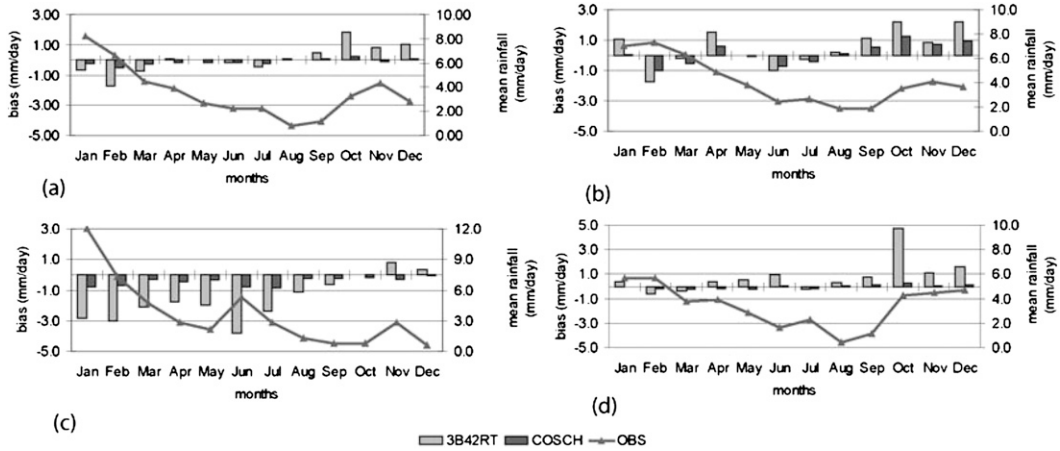

FIG. 5. (left axis) Mean monthly bias in precipitation (mm day^{-1}) as a function of the time of the year shown as dark gray bars for the SALDAS data relative to observations and as light gray bars for the raw TRMM 3B42RT precipitation product relative to observations. (right axis) The solid line is the averaged monthly precipitation for all available stations. Results are given for (a) South America as a whole and for the (b) NO, (c) NE, and (d) CE regions illustrated in Fig. 4.

GOES data, because the Eta model parameterization is known to underestimate cloud cover and consequently to overestimate the downward shortwave radiation reaching the surface.

c. *Temperature and specific humidity*

Figures 9 and 10 show the bias and standard deviation between SALDAS data and observations for 2-m temperature and specific humidity for South America as a whole and for the three separate regions (NO, NE, and SC). The results for monthly-mean daily temperature (Fig. 9) vary between regions, with least bias and RMSE in the NO region and most in the NE region. In the NO region, the bias in temperature is small and has little seasonality because there is little annual variation in temperature. In the semiarid NE and subtropical CS regions, there is a clear seasonality in the bias and a negative bias during the austral winter. The overall bias in temperature integrated over the whole continent reflects this seasonal dependency with mean monthly values reaching 2 K.

SALDAS near-surface specific humidity data consistently overestimates observations by about 2–3 g kg^{-1} in the NE and NO regions throughout the year but consistently underestimates observations by about 1–2 g kg^{-1} in the CS region. SALDAS specific humidity data is taken directly from the South American Regional Reanalysis, and Kalnay et al. (1996) classified reanalysis fields in

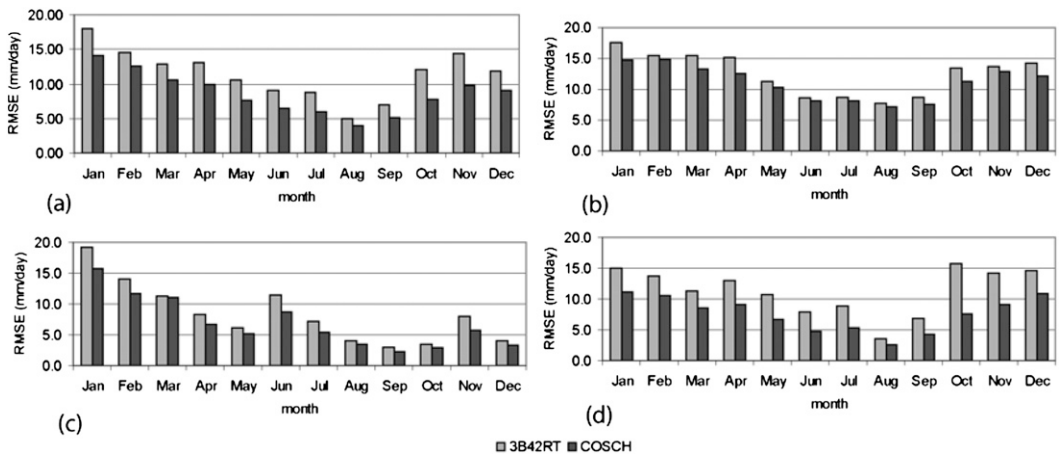

FIG. 6. Monthly-mean RMSE in precipitation shown as dark gray bars for the SALDAS data relative to observations and as light gray bars for the raw TRMM 3B42RT precipitation product relative to observations. Results shown as in Fig. 5.

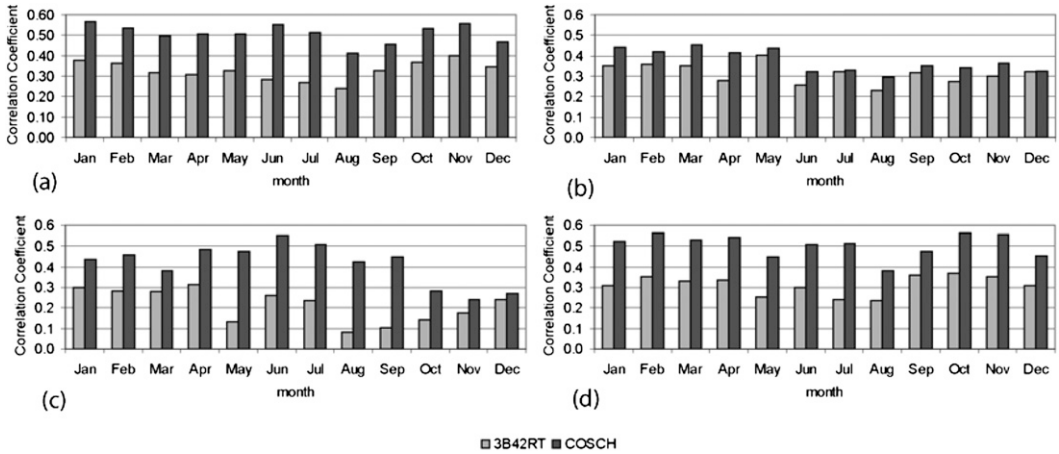

FIG. 7. The correlation coefficient between SALDAS precipitation data and observations (shown as dark gray bars) and between the raw TRMM 3B42RT precipitation data and observations (shown as light gray bars). Results are shown as in Fig. 5.

accordance with the relative influence of the observational data and the model on calculated variable. They considered specific humidity to be a class "B" variable; that is, a variable on which the model has a very strong influence on the analyzed value. Consequently, the consistent overestimation of specific humidity in the SARR (and therefore SALDAS) data may well be related to shortcomings in the SARR atmospheric water distribution calculated by the Eta Model. Yucel et al. (1998) made comparison between Eta Model derived values

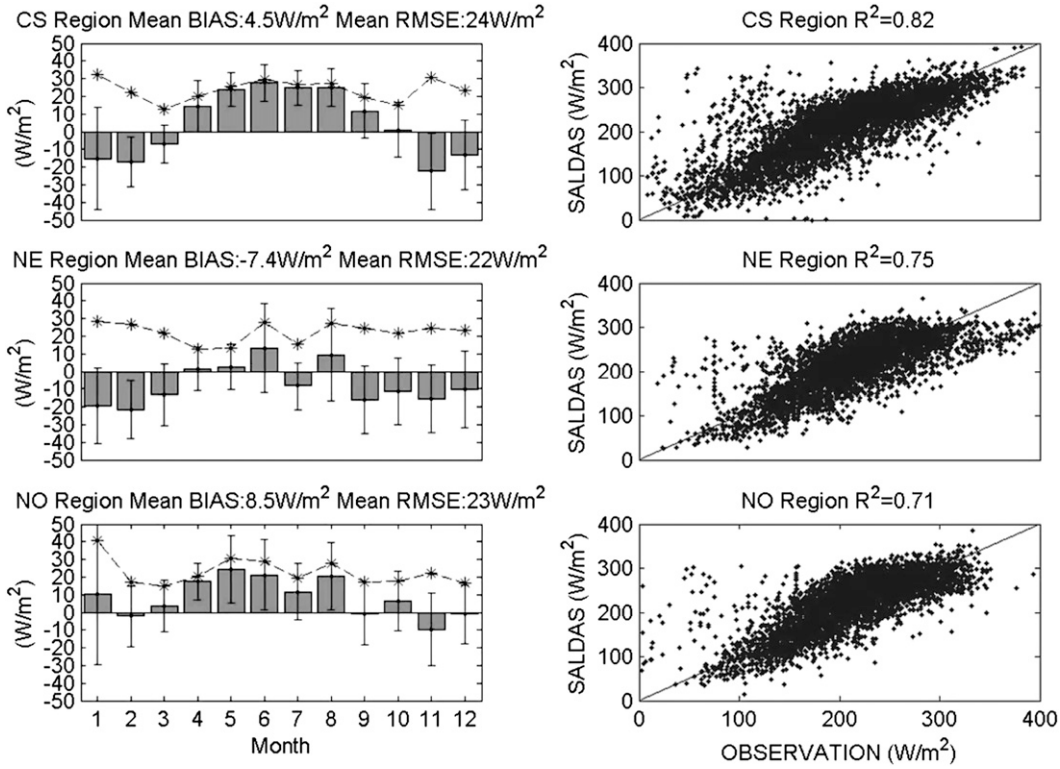

FIG. 8. (left) The mean monthly bias in downward shortwave radiation of the SALDAS data relative to observations during 2004 (shaded bars) with the standard deviation in this bias (error bars). The equivalent RMSE for each month is shown as a dashed line. (right) The correlation coefficient between daily values of shortwave radiation in the SALDAS dataset and observed values. Values are given for the (top) CS, (middle) NE, and (bottom) NO regions.

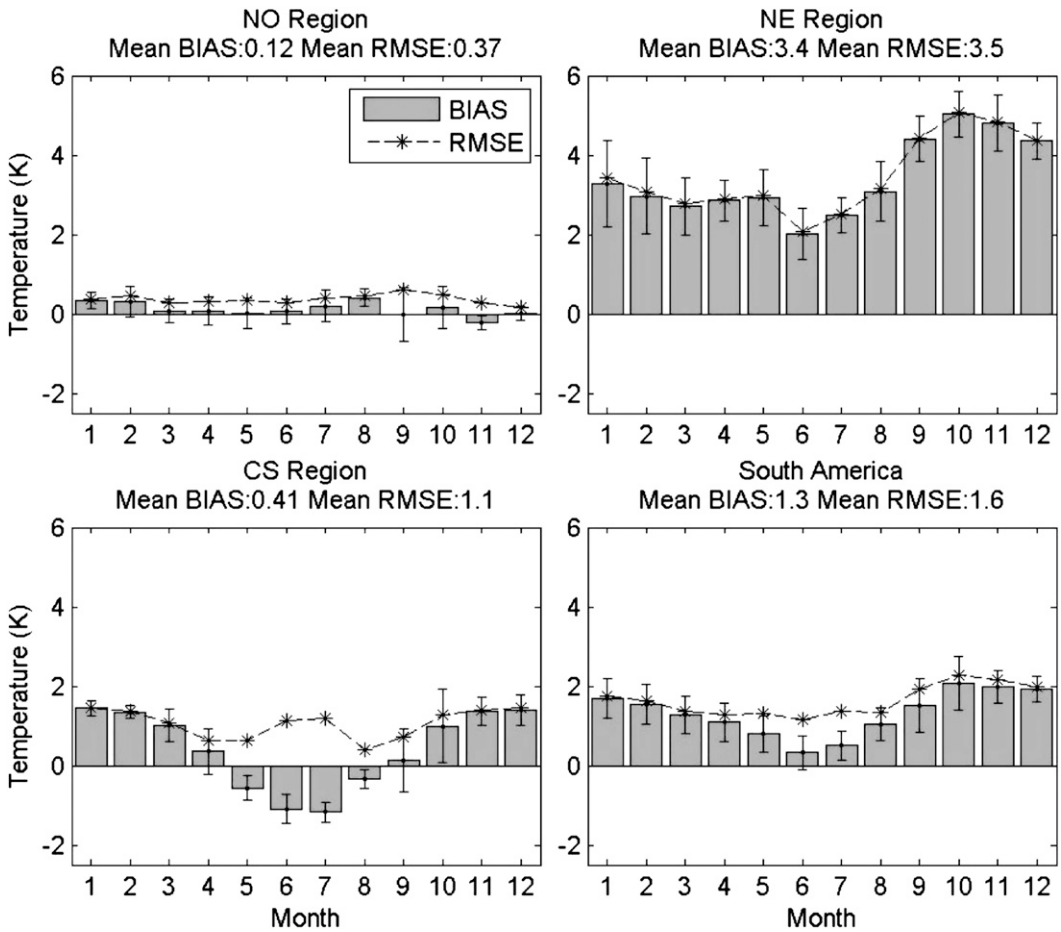

FIG. 9. Mean monthly bias in 2-m temperature of the SALDAS data relative to observations during 2004 (shaded bars) with the standard deviation in this bias (error bars). The equivalent RMSE for each month is shown as a dashed line. Values are given for the (top left) NO, (top right) NE, and (bottom left) CS regions, and for (bottom right) South America as a whole.

and observations and showed coding errors in the Eta Model's postprocessors used to diagnose near-surface temperature and humidity. This same version of the Eta Model was used in the SARR. The near-surface specific humidity biases can also arise from weaknesses in the parameterization of the atmospheric boundary layer that control the redistribution of moisture from surface evaporation to higher levels.

4. Summary

A 5-yr, 0.125°, 3-hourly atmospheric forcing dataset was derived across the South America continent in support of the South American Land Data Assimilation System (SALDAS) initiative. It can be used for a variety of applications, including initiating weather and climate simulations and water management. The resulting product is a composed of data from the South American Regional Reanalysis (SARR) supplemented by precipitation and downward shortwave radiation fields derived from remotely sensed data merged with surface observations. The quality of the forcing datasets was evaluated against available surface observations to the extent feasible given the limited observing network in South America. There are regional differences in the biases for all variables. Volumetric biases in precipitation were typically of the order 0–1 mm day^{-1} and RMSE between 5 and 15 mm day^{-1}. There is a bias in surface solar radiation typically of the order 10 W m^{-2} with an RMSE of the order 20 W m^{-2}. The SALDAS dataset has a positive bias in temperature typically between 0 and 4 K, and a positive bias in near-surface specific humidity around 2–3 g kg^{-1} in tropical regions but a negative bias around 1–2 g kg^{-1} farther south.

Acknowledgments. This study was supported by the NASA–LBA Ecology (Group CD36) Project under Grant NNX06AG91G and the NASA Postdoctoral

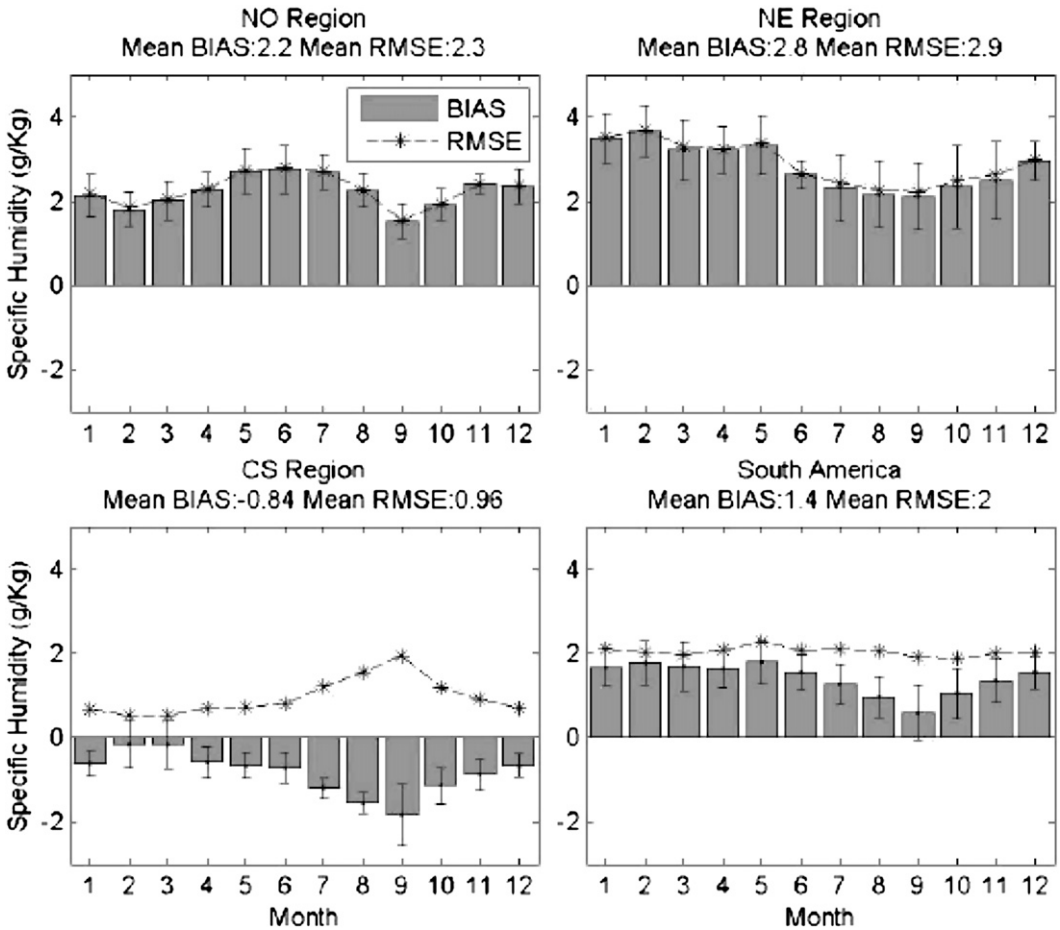

FIG. 10. Same as Fig. 9 but for 2-m specific humidity.

Program under the Oak Ridge Associated Universities (ORAU). Partial support was given by the NASA Terresterial Hydrology Program under Grant NNX08AE50G. The authors would also like to acknowledge James V. Geiger from the NASA Land Information System Team for his kind support.

REFERENCES

Aravéquia, J. A., D. L. Herdies, L. F. Sapucci, R. V. Andreoli, S. F. S. Ferreira, and L. G. G. Gonçalves, 2008: Regional reanalysis 2000-2004 over South America using the RPSAS/ETA model: Experiment description and derived products (in Portuguese). *Bull. Braz. Meteor. Soc.,* **32,** 71–74.

Betts, A. K., J. H. Ball, A. C. M. Beljaars, M. J. Miller, and P. A. Viterbo, 1996: The land surface-atmosphere interaction: A review based on observational and global modeling perspectives. *J. Geophys. Res.,* **101** (D3), 7209–7225.

Bryan, K., 1969: A numerical method for the study of the circulation of the World Ocean. *J. Comput. Phys.,* **4,** 347–376.

Chen, M., P. Xie, J. E. Janowiak, and P. A. Arkin, 2002: Global land precipitation: A 50-yr monthly analysis based on gauge observations. *J. Hydrometeor.,* **3,** 249–266.

——, W. Shi, P. Xie, V. B. S. Silva, V. E. Kousky, R. Wayne Higgins, and J. E. Janowiak, 2008: Assessing objective techniques for gauge-based analyses of global daily precipitation. *J. Geophys. Res.,* **113,** D04110, doi:10.1029/2007JD009132.

Ceballos, J. C., M. J. Bottino, and J. M. de Souza, 2004: A simplified physical model for assessing solar radiation over Brazil using GOES 8 visible imagery. *J. Geophys. Res.,* **109,** D02211, doi:10.1029/2003JD003531.

Chou, S. C., and D. L. Herdies, 1996: Test runs using NCEP Eta model over South America. Preprints, *15th Conf. on Weather Analysis and Forecasting,* Norfolk, VA, Amer. Meteor. Soc., 5.5, 174–175.

——, J. F. Bustamante, and J. L. Gomes, 2005: Evaluation of Eta Model seasonal precipitation forecasts over South America. *Nonlinear Processes Geophys.,* **12,** 537–555.

Cosgrove, B. A., and Coauthors, 2003: Real-time and retrospective forcing in the North American Land Data Assimilation System (NLDAS) project. *J. Geophys. Res.,* **108,** 8842, doi:10.1029/2002JD003118.

de Goncalves, L. G. G., W. J. Shuttleworth, S. C. Chou, Y. Xue, P. R. Houser, D. L. Toll, J. Marengo, and M. Rodell, 2006a: Impact of different initial soil moisture fields on Eta model weather forecasts for South America. *J. Geophys. Res.,* **111,** D17102, doi:10.1029/2005JD006309.

——, ——, B. Nijssen, E. J. Burke, J. A. Marengo, S. C. Chou, P. Houser, and D. L. Toll, 2006b: Evaluation of model-derived and remotely sensed precipitation products for continental South America. *J. Geophys. Res.,* **111,** D16113, doi:10.1029/2005JD006276.

Fennessey, M. J., and J. Shukla, 1999: Impact of initial soil wetness on seasonal atmospheric prediction. *J. Climate,* **12,** 3167–3180.

Huffman, G. J., and Coauthors, 2007: The TRMM Multisatellite Precipitation Analysis (TMPA): Quasi-global, multiyear, combined-sensor precipitation estimates at fine scales. *J. Hydrometeor.,* **8,** 38–55.

Kalnay, E., and Coauthors, 1996: The NCEP/NCAR 40-Year Reanalysis Project. *Bull. Amer. Meteor. Soc.,* **77,** 437–471.

Koster, R. D., and M. J. Suarez, 1999: A simple framework for examining the interannual variability of land surface moisture fluxes. *J. Climate,* **12,** 1911–1917.

——, and Coauthors, 2004: Realistic initialization of land surface states: Impacts on subseasonal forecast skill. *J. Hydrometeor.,* **5,** 1049–1063.

Liou, K.-N., 1980: *An Introduction to Atmospheric Radiation.* Academic Press, 392 pp.

Maurer, E. P., A. W. Wood, J. C. Adam, D. P. Lettenmaier, and B. Nijssen, 2002: A long-term hydrologically based dataset of land surface fluxes and states for the conterminous United States. *J. Climate,* **15,** 3237–3251.

Mesinger, F., T. L. Black, and Z. I. Janjić, 1988: A summary of the NMC step-mountain (Eta) coordinate model. *Proc. Workshop on Limited-Area Modeling Intercomparison,* Boulder, CO, National Center for Atmospheric Research, 91–98.

Mitchell, K. E., and Coauthors, 2004: The multi-institution North American Land Data Assimilation System (NLDAS): Utilizing multiple GCIP products and partners in a continental distributed hydrological modeling system. *J. Geophys. Res.,* **109,** D07S90, doi:10.1029/2003JD003823.

Pinker, R. T., I. Laszlo, and B. Zhang, 2001: Pathfinder large scale radiative fluxes: Data availability and their use in climate research. *IRS 2000: Current Problems in Atmospheric Radiation,* W. L. Smith and Y. M. Timofeyev, Eds., A. Deepak Publishing, 481–484.

Rodell, M., and Coauthors, 2004: The Global Land Data Assimilation System. *Bull. Amer. Meteor. Soc.,* **85,** 381–394.

Row, L. W., D. A. Hastings, and P. K. Dunbar, 1995: *TerrainBase: Worldwide Digital Terrain Data Documentation Manual.* National Geophysical Data Center, Boulder, CO, CD-ROM.

Stackhouse, P. W., S. K. Gupta, S. J. Cox, M. N. Chiacchio, and J. C. Mikovitz, 2001: The WCRP/GEWEX Surface Radiation Budget Project release 2: An assessment of surface flux at 1 degree resolution. *IRS 2000: Current Problems in Atmospheric Radiation,* W. L. Smith and Y. M. Timofeyev, Eds., A. Deepak Publishing, 485–488.

Vila, D., L. G. G. de Goncalves, D. L. Toll, and J. R. Rozante, 2009: Statistical evaluation of combined daily gauge observations and rainfall satellite estimates over continental South America. *J. Hydrometeor.,* **10,** 533–543.

Whitlock, C. H., and Coauthors, 1995: First global WCRP shortwave surface radiation budget dataset. *Bull. Amer. Meteor. Soc.,* **76,** 905–922.

Yucel, I., W. J. Shuttleworth, J. Washburne, and F. Chen, 1998: Evaluating NCEP Eta model-derived data against observations. *Mon. Wea. Rev.,* **126,** 1977–1991.